Psychiatry Research: Neuroimaging 329 (2023) 111583

Contents lists available at ScienceDirect

Psychiatry Research: Neuroimaging

journal homepage: www.elsevier.com/locate/psychresns

Recurrence quantification analysis of periodic dynamics in the default mode network in first-episode drug-naïve schizophrenia

Yafei Kang [a,#], Youming Zhang [b,#], Kexin Huang [c], Zhenhong Wang [a,*]

[a] Shaanxi Provincial Key Research Center of Child Mental and Behavioral Health, School of Psychology, Shaanxi Normal University, Xi'an, China
[b] Department of Radiology, Xiangya Hospital, Central South University, Changsha, China
[c] West China Biomedical Big Data Centre, West China Hospital, Sichuan University, Chengdu, Sichuan, China

ARTICLE INFO

Keywords:
Schizophrenia
Functional magnetic resonance images
Recurrence quantification analysis
Cross recurrence quantification analysis

ABSTRACT

Abnormal functional connectivity (FC) within the default model network (DMN) in schizophrenia has been frequently reported in previous studies. However, traditional FC analysis was mostly linear correlations based, with the information on nonlinear or temporally lagged brain signals largely overlooked. Fifty-five first-episode drug-naïve schizophrenia (FES) patients and 53 healthy controls (HCs) underwent resting-state functional magnetic resonance imaging scanning. The DMN was extracted using independent component analysis. Recurrence quantification analysis was used to measure the duration, predictability, and complexity of the periodic processes of the nonlinear DMN time series. The Mann–Whitney U test was conducted to compare these features between FES patients and HCs. The support vector machine was applied to discriminate FES from HCs based on these features. Determinism, which means predictability of periodic process activity, between the ventromedial prefrontal cortex (vMPFC) and posterior cingulate and between the vMPFC and precuneus, was significantly decreased in FES compared with HCs. Determinism between the vMPFC and precuneus was positively correlated with category fluency scores in FES. The classifier achieved 77% accuracy. Our results suggest that synchronized periodicity among DMN brain regions is dysregulated in FES, and the periodicity in BOLD signals may be a promising indicator of brain functional connectivity.

1. Introduction

Schizophrenia (SZ) is a severe mental disorder with impaired cognition, perception, thought processes, and behaviors (Tandon et al., 2013). However, the etiology and neuropathophysiological mechanism of SZ remain unclear. It has been widely recognized as a dysconnection syndrome (Friston et al., 2016). The dysconnection hypothesis suggests the core pathology of SZ is an aberrant neuromodulation of synaptic plasticity, leading to abnormal functional integration of brain processes, i.e., dysconnectivity. Most direct evidence supporting the dysconnectivity hypothesis comes mainly from resting-state functional magnetic resonance images (fMRI) studies, which have reported widespread functional dysconnectivity between brain regions in SZ (Dong et al., 2018; Venkataraman et al., 2012). Resting state functional connectivity (FC) is an analytical correlation-based method to measure the temporal linear dependence of spontaneous BOLD signals among spatially distributed brain regions and is widely used to help understand brain function in disease and health (Woodward and Cascio, 2015). Considering the brain as a complex nonlinear dynamic system (Vyas et al., 2020), however, this approach is largely insensitive to the nonlinear and temporally lagged dynamics within fMRI signals (Hlinka et al., 2011). Dynamic-based methods have the potential to improve the understanding of functional alterations caused by brain diseases. Compared to static analysis, dynamic analysis may provide additional important information about the profile of brain activity (Du et al., 2017). It is important to explore new methods to examine the temporal organization of fMRI signals, which could contribute to a more accurate characterization of brain connectivity.

Recurrences are basic features of dynamic systems, defined as the repeated occurrence of a state in a dynamic system over time. Recurrence plot (RP) is a nonlinear tool to measure the recurrence characteristics of time series (Marwan et al., 2007). Recurrence quantification analysis (RQA) is used to illustrate the characteristics of a RP and provide a quantitative description of the degree to which brain activity in a

* Corresponding author.
E-mail addresses: vikkihuangkexin@163.com (K. Huang), wangzhenhong@snnu.edu.cn (Z. Wang).
# Yafei Kang and Youming Zhang contributed equally to this work.

https://doi.org/10.1016/j.pscychresns.2022.111583
Received 21 September 2022; Received in revised form 17 December 2022; Accepted 20 December 2022
Available online 23 December 2022

given region displays similar patterns over time. RQA is sensitive to nonlinear and time lagged signal dynamics that have been overlooked in traditional FC studies. By computing cross recurrence plots (CRP), this method can be extended to allow quantification of recurrent signal patterns between two brain regions, named cross RQA (CRQA) (Wallot, 2019). In recent years, RQA has been widely used to analyze physiological signals, such as EEG signals (Heunis et al., 2018; Timothy et al., 2017) and electromyography signals (Jikang et al., 2002). Recently, Curtin et al. applied RQA and CRQA to resting-state fMRI data (Curtin et al., 2022). Using these innovative methods, they found overall atypical default mode network (DMN) connectivity in dizygotic twins with autism disorder. Moreover, Pentari et al. found CRQA to be more sensitive than static functional connectivity and established dynamic functional connectivity in detecting signs of aberrant functional connectivity between brain regions (Pentari et al., 2022). This nonlinear method provides a great opportunity for exploring the hidden patterns and relationships in BOLD signals, which helps researchers better understand the neural mechanism from a new perspective of dynamic functional activities.

Previous studies have consistently reported dysfunctions of the DMN in SZ (Fan et al., 2022; Hu et al., 2017; Wang et al., 2015). Brain regions comprising this resting state network include the ventromedial prefrontal cortex (vMPFC), posterior cingulate cortex (PCC), precuneus, and bilateral angular, whose activity is low when the mind is engaged in specific behavioral tasks and high during spontaneous, self-projecting mental activities (Whitfield-Gabrieli and Ford, 2012). Previous resting state fMRI studies have reported abnormal functional connectivity between constituent DMN brain regions as a key feature of schizophrenia (Fan et al., 2019; Hu et al., 2017). Task-based neuroimaging studies have consistently reported abnormal activity of the DMN in SZ during a broad range of cognitive tasks, such as language (Jeong and Kubicki, 2010; Zhou et al., 2016). Several task-related fMRI studies demonstrated that impaired working memory in SZ may be associated with the abnormal connectivity and activity of the DMN (Godwin et al., 2017; Kim et al., 2009). Furthermore, Sambataro et al. found treatment with olanzapine in SZ patients was associated with increased DMN connectivity (Sambataro et al., 2010). These results suggest that the DMN plays an important role in the physiopathology of SZ. It is necessary to explore the dynamic features of the DMN to obtain more comprehensive insight into how SZ affects the DMN.

Recently, an increasing number of studies have been conducted on machine learning methods for mental diseases (Chen et al., 2022; Meyer et al., 2017). Support vector machine (SVM) has good classification performance in dealing with small sample data (Suthaharan, 2016). It is widely used to establish classification models based on MRI features in mental diseases, including SZ disorders. Whether the RQA/CRQA-related measures could be used as biomarkers for classifying FES patients and HCs was explored in this study.

In the present study, we conducted RQA and CRQA to capture recurrent dynamic characteristics of fMRI signals extracted from regions of the DMN in FES patients and HCs. Then, we explored the relationships between abnormal dynamic measures and impaired cognitive functions in FES. Finally, we used SVM algorithms to differentiate FES patients from HCs using these dynamic measures.

2. Materials and methods

2.1. Subjects

This study was approved by the Ethics Committee of Shanghai Mental Health Center. Written informed consent was obtained from all subjects before participating in the study.

The study recruited 55 FES from the Shanghai Mental Health Center and 53 age-, sex-, and education time-matched HCs recruited by advertisement from the local community. The first-episode drug-naïve schizophrenia patients were recruited the first time when they were seeking help because of psychotic symptoms and did not take any antipsychotic drugs. Patients were included if they had an acute psychotic syndrome, that met the Structured Clinical Interview for DSM-IV Patient version (SCID-I/P), as assessed by two independent experienced psychiatrists. These patients were followed for three months as inpatients after admission and excluded if the second 3-month evaluation was not consistent in diagnosing SZ. The severity of symptoms in FES patients was assessed using the scale for the assessment of negative symptoms (SANS) rating scale and the brief psychiatric rating scale (BPRS) scores. To verify the absence of psychiatric illnesses in the HCs and their first-degree relatives, all HCs were administered the SCID, Non-Patient Edition (SCID-I/NP). Inclusion criteria for patients were a first episode illness, antipsychotic-naïve status, and age between 16 and 40 years. Exclusion criteria were major medical or neurological illness, current pregnancy, a history of suicide risk, and/or alcohol or drug abuse. Additional exclusion criteria for HCs included a current or past history of mental health problems, acquired brain injury or intellectual disability, and the presence of psychosis in any first-degree relatives.

2.2. Cognitive function measure

All subjects received an assessment of cognition functions using the MATRICS Consensus Cognitive Battery (MCCB) (August et al., 2012). This battery is composed of nine subtests across seven domains: 1) Speed of Processing: Trail Making Test-Part A (TMT-A), BACS: Brief Assessment of Cognition in Schizophrenia (BACS), and Category Fluency; 2) Working Memory (WM): Wechsler Memory Scale (WMS); 3) Verbal Learning: Hopkins Verbal Learning Test-Revised (HVLT-R); 4) Visual Learning: Brief Visuospatial Memory Test-Revised (BVMT-R); 5) Reasoning and Problem Solving: Neuropsychological Assessment Battery, mazes subtest (NABMazes); 6) Attention: Continuous Performance Test-Identical Pairs version (CPT-IP); and (7) Social Cognition: The Mayer–Salovey–Caruso Emotional Intelligence Test (MSCEIT).

2.3. Magnetic resonance imaging acquisition

Functional magnetic resonance images were obtained on a 3.0 Tesla Siemens MRI scanner. During data acquisition, the subjects were asked to stay still in the scanner, keeping their eyes closed while staying awake. Resting-state fMRI data were acquired using an echo planar imaging sequence with the following parameters: 170 volumes; repetition time [TR] = 3000 ms; echo time [TE] = 30 ms; slice thickness = 3 mm; sagittal slices = 45; field of view [FOV] = 192 × 192 mm^2; FOV phase = 100%; data matrix size = 64 × 64; voxel size = 3.0 mm × 3.0 mm × 3.0 mm.

2.4. Data preprocessing

fMRI data were preprocessed using the Data Processing & Analysis for Brain Imaging (DPABI) toolbox version 6.1 (Yan et al., 2016). For each subject, the data from the first five time points were removed for magnetic saturation. The fMRI data were then corrected for slice timing and head motion. Three FES patients and 2 HCs were excluded for more than 3 mm maximum head motions or 3 degrees of rotation in any direction. Fifty-two FES patients and 51 HCs were included in the final analysis. Nuisance signals, including 6 motion parameters, white matter, cerebrospinal fluid and global signal, were regressed for each subject. Finally, the fMRI images were normalized to the Montreal Neurological Institute (MNI) space. After preprocessing, we carried out the following series of analyses.

2.5. Independent component analysis

The preprocessed fMRI images were decomposed into different brain networks using group independent component analysis (ICA) within the group ICA of the fMRI toolbox (GIFT 3.0, http://icatb.sourceforge.net)

(Rachakonda et al., 2007). We first estimated the number of independent components (ICs) of the fMRI data for all subjects using the "Minimum description length" criterion. The number of ICs estimated was 30. Second, to decrease the computational complexity, data reduction was employed using two rounds of principal component analysis. Finally, the ICs were estimated by the fast ICA algorithm. The corresponding time course and spatial z-map for each subject as well as the time course and average z-map for all subjects were obtained for each component. With regard to IC selection, we correlated each of the 20 ICs with the DMN network templates from Stanford's Functional Imaging in the Neuropsychiatric Disorders (FIND) Laboratory, and the ICs with the highest correlation coefficient were selected. Spherical regions of interest (ROIs) were defined in a 6 mm radius around the coordinates of the peak voxels of the brain regions in the selected ICs. As with previous studies, the selected masks were vMPFC (-6, 53 34), PCC (-5, -52, 32), precuneus (4, -59, 32), left angular (-54, -60, 27), and right angular (59, -57, 29).

Before ROI time course extraction, we conducted postprocessing steps on the preprocessed fMRI images. Several covariates, such as 24-head motion parameters and the mean time series of white matter and cerebrospinal fluid, were removed from the imaging data. A temporal bandpass filter (0.01–0.1 Hz) was applied to minimize the effects of cardiac and respiratory fluctuations. Then, spatial smoothing was conducted with a Gaussian kernel of 6 mm full-width at half-maximum. The mean time course in each ROI was extracted from the postprocessed images by averaging the time courses of all voxels in the ROI.

2.6. Recurrence quantification analysis

Consistent with previous studies (Curtin et al., 2022; Pentari et al., 2022), the conduction of RQA involves three general steps of analysis, which here were applied in the context of BOLD signals extracted from regions of the DMN networks (Figure 1 a, b and c). First, to construct phase portraits, the time delay embedding method was used to reconstruct a multidimensional state space from the one-dimensional series (Figure 1d). This process includes the specification of two parameters, τ (embedding time delay) and m (embedding dimensions), which determine the lag interval and number of dimensions used in the reconstruction, respectively. Using the mutual information algorithm, the τ parameter was set individually for each time series data and was regarded as the first minimum of the mutual information function. The m parameter was determined through the conduction of a false nearest-neighbors algorithm; specifically, the smallest value of m that minimized the number of false nearest neighbors was selected.

Then, the resulting phase portraits were used to construct a RP through the iterative application of a threshold ε to each point in the phase portrait (Figure 1e). As in previous studies, the ε parameter in the present study was set via a dynamic filter to yield a fixed recurrence rate of 10% (Austin et al., 2019; Curtin et al., 2020).

Finally, the RQA descriptors were calculated based on the location and number of recurrence points on the RP. In this study, we derived three metrics: determinism (DET), maximal diagonal line length (MDL), and entropy of the diagonal line lengths (ENT) (Figure 1f). DET evaluates the percentage of recurrence points forming diagonals from all recurrence points and is related to the time series predictability. MDL is used to quantify the duration of periodic processes. ENT is used to measure the amount of information contained in the RP. The RQA analysis was conducted with the Recurrence Plot Toolbox in MATLAB 2016a (Chen and Yang, 2012).

By computing CRP, the application of univariate (nodal) RQA to individual ROIs signals was then extended to quantify synchronization between ROIs via the conduction of CRQA, which, as in RQA, yields measures of DET, MDL, and ENT of cross-signal synchronization. The CRQA analysis was performed with the Cross-Recurrence Toolbox (Meyers et al., 2020; Yang, 2011) in MATLAB 2016a.

Menon proposed a triple network model to study the disruption of functional connectivity in psychopathology in psychiatric disorders (Menon, 2011). Three networks, DMN, central executive network (CEN), and the salience network (SN), are included in the triple network model. In consideration of the SN and central CEN are closely related to the DMN. We also explored the periodic processes of these two networks using same method. The detailed information about this section was showed in supplement materials, please see Table S1 to Table S5.

2.7. Statistical analyses

2.7.1. Comparison of MCCB scores and RQA/CQRA measures between groups

Group differences in age and years of education were compared using independent two-sample *t tests*. A chi-square test was conducted to compare gender distributions. Statistical differences in MCCB scores between FES patients and HCs were identified using general linear model (GLM) analysis with age, sex, and years of education as covariates.

We used the Mann−Whitney U test to assess whether the RQA/CRQA measures were different between the FES and HC groups. We applied

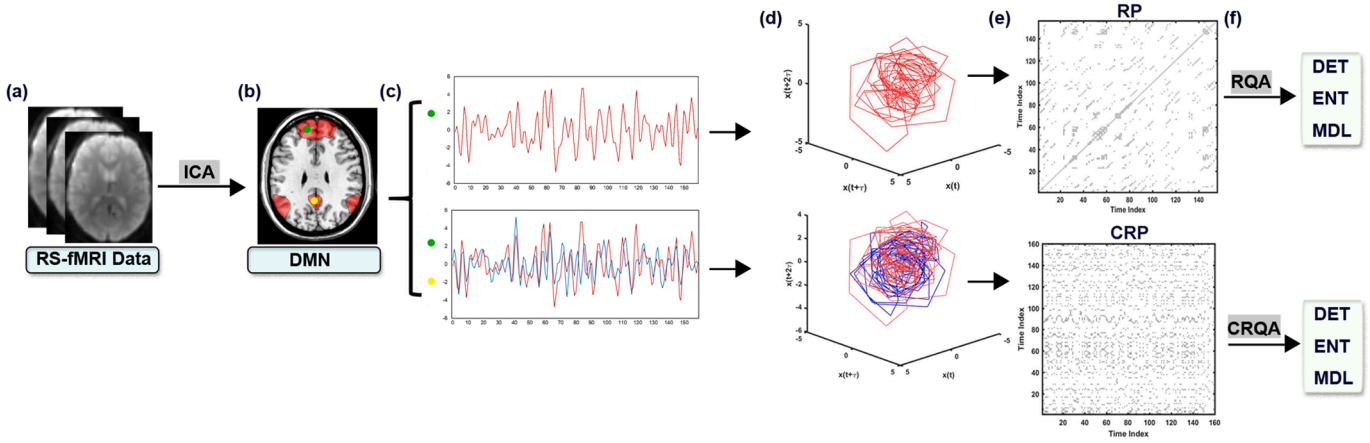

Fig. 1. Flowchart of the study. (a)Resting-state fMRI data preprocessing. (b)The key regions of DMN were identified by ICA analysis. (c)Example of BOLD signals of brain regions in DMN. (d) The trajectory of the state vectors is formed in phase space of BOLD signals of DMN regions. (e) Recurrence plot derived from phase space. (f) Finally, the RQA/CRQA related metrics are computed.
DMN: default mode network, RP: recurrence plot, CRP: ross recurrence plot, DET: determinism, ENT: entropy, MDL: mean diagonal length, RQA: recurrence quantification analysis, CRQA: cross recurrence quantification analysis

false discovery rate (FDR) correction to correct the p values for multiple statistical tests.

2.7.2. Brain-behavioral relationship

For the RQA/CRQA indices showing significant intergroup differences (Mann−Whitney U test, $p < 0.05$, FDR corrected), we conducted Pearson's correlation analysis between RQA/CRQA indices and MCCB scores in the FES and HC groups ($p < 0.05$).

2.8. Classification analysis using SVM

We further used RQA/CRQA measures to classify FES patients and HCs using the easylearn toolbox (https://github.com/lichao312214129/easylearn) based on the sklearn package in Python (Pedregosa et al., 2011). First, the features were rescaled to lie within a range of 0 to 1 by the min-max normalization method. We used a nested 10-fold cross-validation (CV) method. Here, the inner CV loop is employed to fit, tune and select the optimal parameters of the classifier, and the external CV is used to estimate the performance of the classifier. A support vector machine with the polynomial kernel was used as a classifier in our study. Support vector machine recursive feature elimination (SVM-RFE) algorithm was used to select the most discriminative feature set in the training set of the inner CV loop. The SVM-REF method is an iterative backward selection algorithm that recursively removes features with lower ranking scores until the optimal feature set remains. Briefly, the process of this method is described as follows: 1) train the SVM classifier; 2) compute the weight values of features; 3) rank the features from the minimum to the maximum by square weight values; 4) update the feature ranking list; 5) eliminate the lowest-ranked feature, and then repeat these processes until all of the features are ranked. Once we obtained the highest classification accuracy in the inner CV loop, we defined the optimal classification model. Subsequently, this classification model was adopted in the training set of the external CV for the final classification. The resulting report was the average accuracy of 10 repetitions of tenfold CV. Sensitivity, specificity, and area under the receiver operating characteristic (ROC) curve (AUC) were calculated as supporting measures for performance evaluation.

3. Results

3.1. Demographic and cognitive performance data

Our sample consisted of 52 FES patients and 51 age-, sex-, and years of education-matched HCs. For a detailed description of the subjects, please see Table 1.

The index scores and total scores of the MCCB were compared between the FES patients and HCs, as shown in Table 2. Except for a nonsignificant difference in the CPT-IP ($p = 0.106$) and significantly higher TMT-A and MSCEIT scores in FES patients, the cognitive scores on the MCCB tests and total scores were significantly lower in FES patients than HCs ($p < 0.05$).

Table 1
Demographic and clinical characteristics of FES and HCs

Variables	FES (N = 52) Mean±SD	HCs (N = 51) Mean±SD	p
Male/Female	20/32	22/29	0.629
Age(years)	26±6.88	26±6.51	0.798
Education(years)	12.6±2.99	13±2.81	0.626
SANS			
Affect flattening	5.14±5.26		
Alogia	2.21±3.82		
Avolition-apathy	3.87±3.35		
Anhedonia-asociality	5.81±4.58		
Attention	1.81±2.11		
SANS total	18.85±16.23		
BPRS	47±10.32		

FES: first-episode schizophrenia; HCs: healthy controls; SD: standard deviation; SANS: assessment of negative symptoms; BPRS: brief psychiatric rating scale

Table 2
Comparing the cognitive scores from the MATRICS Consensus Cognitive Battery (MCCB) in FES and HCs

Variables	FES Mean±SD	HC Mean±SD	F	P
TMT-A	53.57±11.49	46.36±6.53	17.163	<0.0001***
BACS	45.09±9.06	55.01±8.34	38.95	<0.0001***
HVLT-R	47.84±10.62	52.2±8.90	5.707	0.018*
WMS	46.79±10.00	53.2±8.99	12.187	0.000723***
NABMazes	46.38±10.27	53.68±8.29	18.496	<0.0001***
BVMT-R	46.80±10.57	53.26±8.28	13.968	0.000313***
Category fluency	48.06±10.34	51.98±9.32	4.008	0.048*
CPT-IP	45.94±9.79	54.08±8.63	2.661	0.106
MSCEIT	51.55±12.62	48.43±6.04	23.804	<0.0001***
MCCB total score	47.7±10.71	52.35±8.71	6.183	0.014*

MCCB: MATRICS Consensus Cognitive Battery
TMT: Trail Making Test-Part A;
BACS: Brief Assessment of Cognition in Schizophrenia;
HVLT-R: Hopkins Verbal Learning Test-Revised;
WMS: Wechsler Memory Scale;
NABMazes: Neuropsychological Assessment Battery, mazes subtest;
BVMT-R: Brief Visuospatial Memory Test-Revised;
CPT-IP: Continuous Performance Test-Identical Pairs version
MSCEIT: Mayer–Salovey–Caruso Emotional Intelligence Test
* $p<0.05$; ** $p<0.01$
*** $p<0.001$

3.2. Differences in RQA/CQRA metrics between the FES and HC groups

Tables 3 and 4 show the comparisons between the FES and HCs across the RQA/CRQA-related features. There was no statistically significant difference in RQA-related indices between the FES and HC groups. For the CRQA-related features, the FES patients showed a significant DET reduction relative to the HCs. In detail, the DET values between the vMPFC and PCC ($p = 0.00028$, $Z = -3.628$, Mann−Whitney U test, FDR corrected, Figure 2a) and between the vMPFC and precuneus ($p = 0.00085$, $Z = -3.335$, Mann−Whitney U test, FDR corrected, Figure 2b) were significantly decreased in the FES group compared with the HC group.

3.3. Correlation results

In FES patients, the DET values between the vMPFC and precuneus were positively correlated with the category fluency score before multiple testing correction ($r = 0.409$, $p = 0.003$, Figure 3).

Table 3
Analysis of RQA features between FES and HCs

Measure	ROI	Z	p
DET	vMPFC	-0.422	0.659
	PCC	-2.335	0.0195
	precuneus	-1.098	0.272
	L.angular	-0.432	0.666
	R.angular	-0.241	0.810
ENT	vMPFC	-0.798	0.425
	PCC	-1.84	0.066
	precuneus	-0.343	0.732
	L.angular	-0.02	0.984
	R.angular	-0.732	0.464
MDL	vMPFC	-1.095	0.274
	PCC	-1.530	0.126
	precuneus	-0.887	0.375
	L.angular	-0.155	0.877
	R.angular	-1.540	0.124

DET: determinism, ENT: entropy, MDL: mean diagonal length, vMPFC: ventromedial prefrontal cortex, PCC: posterior cingulate, L: left, R: right

Table 4
Analysis of CRQA features between FES and HCs

Measure	ROI to ROI	Z	p
DET	vMPFC-PCC	**-3.628**	**0.00028**[a]
	vMPFC -precuneus	**-3.335**	**0.0008**[a]
	vMPFC-L.angular	-2.134	0.033
	vMPFC -R.angular	-2.141	0.032
	PCC- precuneus	-1.834	0.067
	PCC- L.angular	-2.015	0.044
	PCC- R.angular	-0.887	0.375
	precuneus- L.angular	-1.30	0.194
	precuneus- R.angular	-1.283	0.199
	L.angular- R.angular	-0.122	0.222
ENT	vMPFC-PCC	-2.164	0.031
	vMPFC -precuneus	-1.26	0.208
	vMPFC-L.angular	-0.224	0.823
	vMPFC -R.angular	-0.125	0.900
	PCC- precuneus	-1.135	0.257
	PCC- L.angular	-1.827	0.068
	PCC- R.angular	-1.405	0.16
	precuneus- L.angular	-0.422	0.673
	precuneus- R.angular	-1.082	0.279
	L.angular- R.angular	-1.649	0.099
MDL	vMPFC-PCC	-2.216	0.027
	vMPFC -precuneus	-1.266	0.205
	vMPFC-L.angular	-2.891	0.004
	vMPFC -R.angular	-2.619	0.008
	PCC- precuneus	-1.174	0.240
	PCC- L.angular	-1.84	0.066
	PCC- R.angular	-1.369	0.171
	precuneus- L.angular	-0.508	0.612
	precuneus- R.angular	-0.825	00.0
	L.angular- R.angular	-1.90	0.057

DET: determinism, ENT: entropy, MDL: mean diagonal length, vMPFC: ventromedial prefrontal cortex, PCC: posterior cingulate cortex, L: left, R: right
[a] FDR corrected

3.4. Classification results

As shown in Figure 4, the SVM classification achieved a statistically significant AUC of 0.82, 75% sensitivity, 78% specificity, and 77% accuracy (p=0.001, permutation test, Figure 4a). We found that DET of the vMPFC-PCC and vMPFC-precuneus, both of which significantly differed between FES patients and HCs, were the top important features in classifying FES patients (Figure 4b).

4. Discussion

Previous studies exploring functional connectivity using correlation-based methods reported alterations of the DMN in SZ patients (Fan et al., 2020; Zhang et al., 2020); unfortunately, the dynamic features involved in these processes are largely overlooked. In the present study, we characterized periodic features of the DMN in FES using a novel analytical method, namely, RQA/CQRA. We found abnormal interdependent periodic processes between DMN regions in FES patients. Using CRQA, we found that DET values between the vMPFC and PCC and between the vMPFC and precuneus were significantly decreased in the FES group compared with the HC group. The DET values between the vMPFC and precuneus were positively correlated with the category fluency scores in FES patients. SVM analysis demonstrated that these dynamic indices could serve as biomarkers for distinguishing FES patients from HCs. No between-group difference was found in the RQA-based features. These findings emphasize that the periodic processes active between DMN regions are dysregulated, which has an influence on the category fluency of FES patients. Moreover, these results indicate that RQA/CRQA may be potential methods for quantifying the dynamic characteristics of BOLD signals.

To our knowledge, this is the first study to conduct RQA/CRQA to measure the periodicity of DMN activity using resting-state fMRI data in SZ. We found decreased DET values between the vMPFC and PCC and

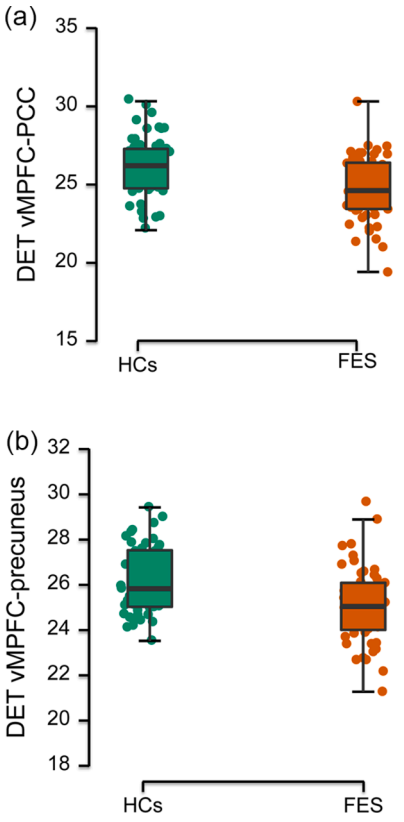

Fig. 2. FES-related dysregulation of DET between vMPFC and PCC (p = 0.00028, Z = -3.628, Mann-Whitney U test, FDR corrected), and between vMPFC and precuneus (p = 0.00085, Z = -3.335, Mann-Whitney U test, FDR corrected).
DET: determinism, vMPFC: ventromedial prefrontal cortex, PCC: posterior cingulate cortex

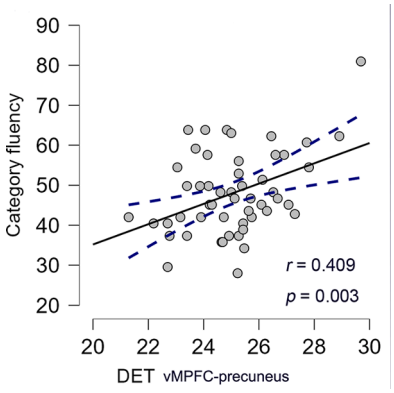

Fig. 3. DET between vMPFC and precuneus showing significant positive correlation with category fluency performance in FES.
DET: determinism, vMPFC: ventromedial prefrontal cortex

between the vMPFC and precuneus in FES patients in comparison to HCs. The vMPFC, PCC, and precuneus are regarded as key hubs of the DMN (Raichle, 2015). DET characterizes the proportion of elements forming long diagonal lines in a given RP. The longer the diagonal lines are, the greater the DET values. A larger value of DET implies that the dynamic functional activities between brain regions are more 'deterministic'. Here, higher 'determinism' means that longer consecutive sequences of functional activities repeat at different times (Araújo et al., 2022). Lower determinism in FES indicates that the connectivity pattern of one region is more difficult to predict by the past connectivity pattern

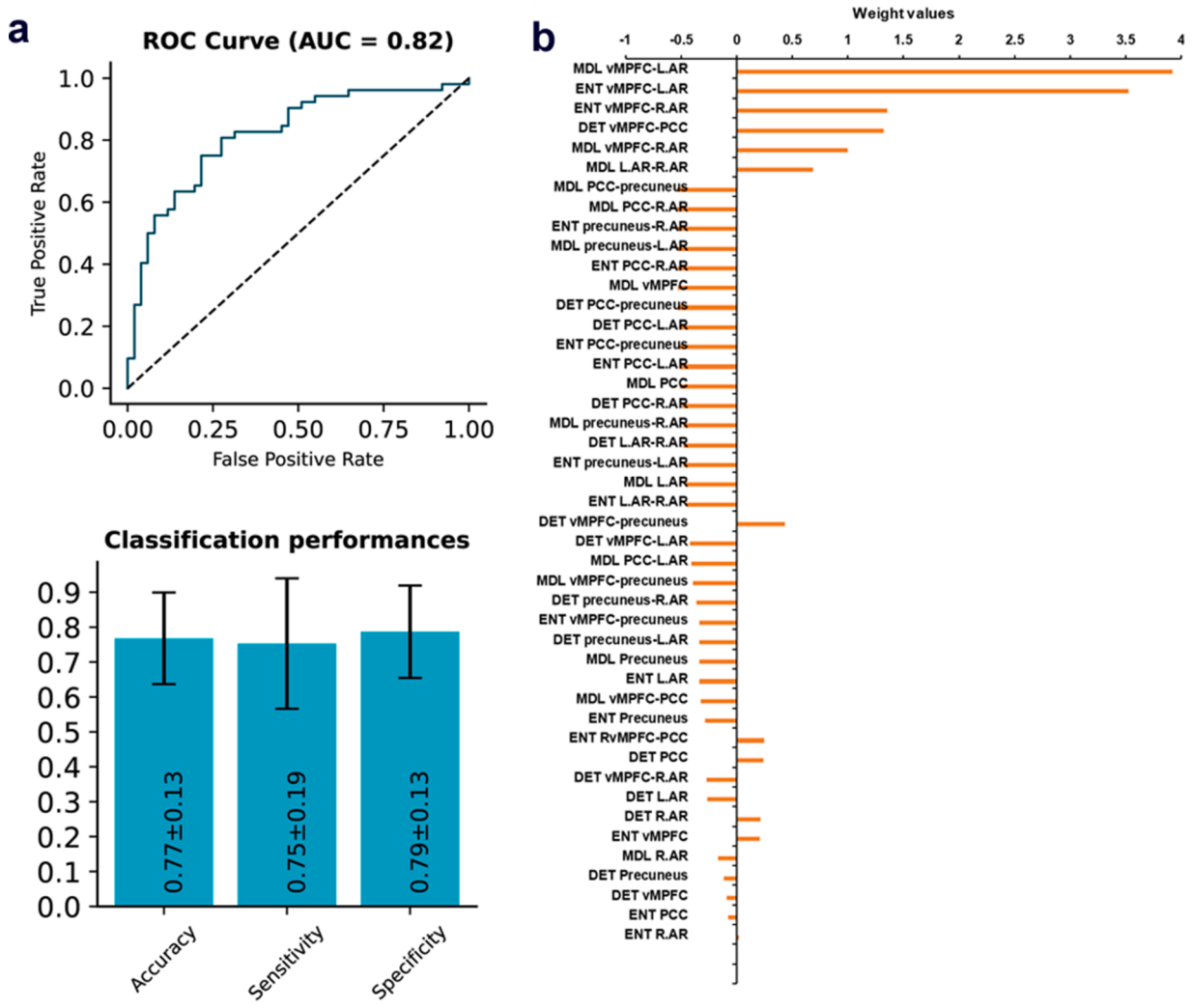

Fig. 4. Classification performance of RQA/CRQA-related features in discrimination between FES patients and HCs. (a) ROC, the accuracy, sensitivity, and specificity of the classification was 0.82, 77.0%, 75%, and 78%, respectively. (b) The region weight in the classification.
RQA: recurrence quantification analysis, CRQA: cross recurrence quantification analysis, ROC: receiver operating characteristic, L.AR: left angular, R.AR: right angular

of the other region, reflecting less predictable and less patterned connectivity between these regions. Previous studies have reported that the DMN consists of separate components that participate in different subfunctions of self-referential processing (Northoff and Bermpohl, 2004; Northoff et al., 2006). The anterior part of the DMN, such as the vMPFC, has been implicated in identifying stimuli as self-relevant by integrating sensory, emotional, and cognitive information (Schmitz and Johnson, 2007). The posterior part of the DMN, such as the precuneus and PCC, has been associated with emotion processing, autobiographic memory, and representation of the external environment (Leech et al., 2011). Interactions between the anterior and posterior DMN play a critical role in processing self-referential information by integrating internal information, external information and autobiographic information about stimuli (Knyazev, 2013; Uddin et al., 2009). Phenomenological studies propose that disturbance of the basic sense of self may be a core feature of SZ (Hur et al., 2014). The DMN has been suggested as a neural system that plays a significant role in the multifaceted experiences of the self (Qin and Northoff, 2011). The abnormal DET values between the vMPFC and PCC and between the vMPFC and precuneus may indicate abnormal functional interactions between the anterior and posterior DMN in FES patients. Aberrant functional interactions of DMN may be closely related to self-disturbance in SZ. We expect that our findings may provide meaningful insights into the pathological mechanism of SZ.

Correlation analysis indicated a positive correlation between the category fluency score and DET values between the vMPFC and precuneus in FES patients. Category fluency impairment is well established in schizophrenia patients (Chen et al., 2000; Snitz et al., 2006; Sumiyoshi et al., 2014). Our study also found that FES patients showed significant category fluency deficits. Category fluency tasks require participants to rapidly generate words based on particular criteria (Vonk et al., 2019), which demands language, semantic memory abilities, and executive functions (Sung et al., 2013). Considerable efforts have been made to understand the neural mechanism of impaired category fluency performance in schizophrenia patients. Ragland et al. found greater activities in the prefrontal, parietal, and anterior cingulate regions during semantic word generation by schizophrenia patients than in HCs (Ragland et al., 2008). In the present study, we found that periodic activity between the vMPFC and precuneus was correlated with category fluency performance in FES. As mentioned above, we found significantly shorter consecutive sequences of functional activity repeats in FES patients, manifested as lower DET values between the vMPFC and precuneus in patients, and the lower DET values corresponded to poor category fluency performance in FES patients. This result indicated that the abnormal consecutive sequences of activities between the vMPFC and precuneus might contribute to impairments in category fluency in FES patients.

In our study, we found that the SVM classifier achieved high accuracy for classifying FES and HCs based on RQA/CRQA-related features. Our findings provide evidence that there is tremendous potential for using machine learning-based methods combined with MRI features to predict SZ. DET values between the vMPFC-PCC and vMPFC-precuneus, both of which significantly differed between FES patients and HCs, were the top important features in classifying FES patients. This result indicated that abnormal dynamic functional activities between these regions paly important role in distinguishing FES from HCs.

Inevitably, the present study has several limitations. First, owing to the limited sample size in this study, our findings need to be interpreted with caution and should be confirmed in larger samples. Second, multiple comparisons were not conducted for correlation analyses between cognitive scores and imaging measures; thus, the correlation results must be interpreted cautiously and there is a need for a large sample of datasets for validation.

In conclusion, this study focuses on the RQA and CRQA as methods for exploring abnormal periodic features of the DMN in FES in the resting state. This study emphasizes the application of nonlinear analytical methods for the exploration of abnormal brain periodic activity using resting-state fMRI data in SZ, and the periodic features of the DMN may serve as biomarkers for distinguishing FES. Moreover, abnormal periodic processes active in the DMN may play an important role in the well-described cognitive impairment in patients with FES.

Role of the funding sources

No funders played a role in the study.

CRediT authorship contribution statement

Yafei Kang: Conceptualization, Methodology, Investigation, Writing – original draft, Writing – review & editing. **Youming Zhang:** Writing – review & editing. **Kexin Huang:** Writing – review & editing. **Zhenhong Wang:** Conceptualization, Writing – review & editing, Supervision.

Declaration of Competing Interest

The authors declare that they have no known competing financial interests or personal relationships that could have appeared to influence the work reported in this paper.

Acknowledgments

This work was supported by the China Postdoctoral Science Foundation (2021M692007), Natural Science Foundation (Youth Science Foundation Project) of Shaanxi Province (2022JQ-875), National Natural Science Foundation of China (82001784). All authors report no biomedical financial interest or potential conflicts of interest.

Supplementary materials

Supplementary material associated with this article can be found, in the online version, at doi:10.1016/j.pscychresns.2022.111583.

References

Araújo, N.S., Reyes-Garcia, S.Z., Brogin, J.A.F., Bueno, D.D., Cavalheiro, E.A., Scorza, C. A., Faber, J., 2022. Chaotic and stochastic dynamics of epileptiform-like activities in sclerotic hippocampus resected from patients with pharmacoresistant epilepsy. PLoS Comput. Biol. 18 (4), e1010027 https://doi.org/10.1371/journal.pcbi.1010027.

August, S.M., Kiwanuka, J.N., McMahon, R.P., Gold, J.M., 2012. The MATRICS consensus cognitive battery (MCCB): clinical and cognitive correlates. Schizophr. Res. 134 (1), 76–82. https://doi.org/10.1016/j.schres.2011.10.015.

Austin, C., Curtin, P., Curtin, A., Gennings, C., Arora, M., Tammimies, K., Isaksson, J., Willfors, C., Bölte, S., 2019. Dynamical properties of elemental metabolism distinguish attention deficit hyperactivity disorder from autism spectrum disorder. Transl. Psychiatry 9 (1), 238. https://doi.org/10.1038/s41398-019-0567-6.

Chen, Q., Bi, Y., Zhao, X., Lai, Y., Yan, W., Xie, L., Gao, T., Xie, S., Zeng, T., Li, J., Kuang, S., Gao, L., Lv, Z., 2022. Regional amplitude abnormities in the major depressive disorder: A resting-state fMRI study and support vector machine analysis. J. Affect. Disord. 308, 1–9. https://doi.org/10.1016/j.jad.2022.03.079.

Chen, Y., Yang, H., 2012. Multiscale recurrence analysis of long-term nonlinear and nonstationary time series. Chaos, Solit. Fract. 45 (7), 978–987. https://doi.org/10.1016/j.chaos.2012.03.013.

Chen, Y.L., Chen, Y.H., Lieh-Mak, F., Lieh, M.F., 2000. Semantic verbal fluency deficit as a familial trait marker in schizophrenia. Psychiatry Res. 95 (2), 133–148. https://doi.org/10.1016/S0165-1781(00)00166-9.

Curtin, P., Austin, C., Curtin, A., Gennings, C., Figueroa-Romero, C., Mikhail, K.A., Botero, T.M., Goutman, S.A., Feldman, E.L., Arora, M., 2020. Dysregulated biodynamics in metabolic attractor systems precede the emergence of amyotrophic lateral sclerosis. PLoS Comput. Biol. 16 (4), e1007773 https://doi.org/10.1371/journal.pcbi.1007773.

Curtin, P., Neufeld, J., Curtin, A., Arora, M., Bölte, S., 2022. Altered periodic dynamics in the default mode network in autism and attention-deficit/hyperactivity disorder. Biol. Psychiatry 91 (11), 956–966. https://doi.org/10.1016/j.biopsych.2022.01.010.

Dong, D., Wang, Y., Chang, X., Luo, C., Yao, D., 2018. Dysfunction of large-scale brain networks in schizophrenia: a meta-analysis of resting-state functional connectivity. Schizophrenia Bull. 44 (1), 168–181. https://doi.org/10.1093/schbul/sbx034.

Du, Y., Pearlson, G.D., Lin, D., Sui, J., Chen, J., Salman, M., Tamminga, C.A., Ivleva, E.I., Sweeney, J.A., Keshavan, M.S., Clementz, B.A., Bustillo, J., Calhoun, V.D., 2017. Identifying dynamic functional connectivity biomarkers using GIG-ICA: application to schizophrenia, schizoaffective disorder, and psychotic bipolar disorder. Hum. Brain Mapp. 38 (5), 2683–2708. https://doi.org/10.1002/hbm.23553.

Fan, F., Tan, S., Huang, J., Chen, S., Fan, H., Wang, Z., Li, C.-S.R., Tan, Y., 2020. Functional disconnection between subsystems of the default mode network in schizophrenia. Psychol. Med. https://doi.org/10.1017/S003329172000416X.

Fan, F., Tan, S., Huang, J., Chen, S., Fan, H., Wang, Z., Li, C.-S.R., Tan, Y., 2022. Functional disconnection between subsystems of the default mode network in schizophrenia. Psychol. Med. 52 (12), 2270–2280. https://doi.org/10.1017/S003329172000416X.

Fan, F., Tan, Y., Wang, Z., Yang, F., Fan, H., Xiang, H., Guo, H., Hong, L.E., Tan, S., Zuo, X.-N., 2019. Functional fractionation of default mode network in first episode schizophrenia. Schizophr. Res. 210, 115–121. https://doi.org/10.1016/j.schres.2019.05.038.

Friston, K., Brown, H.R., Siemerkus, J., Stephan, K.E., 2016. 2016. The dysconnection hypothesis. Schizophr. Res. 176 (2-3), 83–94. https://doi.org/10.1016/j.schres.2016.07.014.

Godwin, D., Ji, A., Kandala, S., Mamah, D., 2017. Functional connectivity of cognitive brain networks in schizophrenia during a working memory task. Front. Psychiatry 8, 294. https://doi.org/10.3389/fpsyt.2017.00294.

Heunis, T., Aldrich, C., Peters, J.M., Jeste, S.S., Sahin, M., Scheffer, C., de Vries, P.J., 2018. Recurrence quantification analysis of resting state EEG signals in autism spectrum disorder - a systematic methodological exploration of technical and demographic confounders in the search for biomarkers. BMC Med. 16 (1), 101. https://doi.org/10.1186/s12916-018-1086-7.

Hlinka, J., Paluš, M., Vejmelka, M., Mantini, D., Corbetta, M., 2011. Functional connectivity in resting-state fMRI: is linear correlation sufficient? Neuroimage 54 (3), 2218–2225. https://doi.org/10.1016/j.neuroimage.2010.08.042.

Hu, M.-L., Zong, X.-F., Mann, J.J., Zheng, J.-J., Liao, Y.-H., Li, Z.-C., He, Y., Chen, X.-G., Tang, J.-S., 2017. A review of the functional and anatomical default mode network in schizophrenia. Neurosci. Bull. 33 (1), 73–84. https://doi.org/10.1007/s12264-016-0090-1.

Hur, J.-W., Kwon, J.S., Lee, T.Y., Park, S., 2014. The crisis of minimal self-awareness in schizophrenia: a meta-analytic review. Schizophr. Res. 152 (1), 58–64. https://doi.org/10.1016/j.schres.2013.08.042.

Jeong, B., Kubicki, M., 2010. Reduced task-related suppression during semantic repetition priming in schizophrenia. Psychiatry Res. 181 (2), 114–120. https://doi.org/10.1016/j.pscychresns.2009.09.005.

Jikang, Z., Zhihuai, S., Weiqiang, H., 2002. Application of recurrence qualification analysis to EMG. Shengwu Wuli Xuebao 18 (2), 241–245.

Kim, D.I., Manoach, D.S., Mathalon, D.H., Turner, J.A., Mannell, M., Brown, G.G., Ford, J.M., Gollub, R.L., White, T., Wible, C., 2009. Dysregulation of working memory and default-mode networks in schizophrenia using independent component analysis, an fBIRN and MCIC study. Hum. Brain Mapp. 30 (11), 3795–3811. https://doi.org/10.1002/hbm.20807.

Knyazev, G.G., 2013. Extraversion and anterior vs. posterior DMN activity during self-referential thoughts. Front. Hum. Neurosci. 6, 348. https://doi.org/10.3389/fnhum.2012.00348.

Leech, R., Kamourieh, S., Beckmann, C.F., Sharp, D.J., 2011. Fractionating the default mode network: distinct contributions of the ventral and dorsal posterior cingulate cortex to cognitive control. J. Neurosci. 31 (9), 3217–3224. https://doi.org/10.1523/JNEUROSCI.5626-10.2011.

Marwan, N., Romano, M.C., Thiel, M., Kurths, J., 2007. Recurrence plots for the analysis of complex systems. Phys. Rep. 438 (5-6), 237–329. https://doi.org/10.1016/j.physrep.2006.11.001.

Menon, V., 2011. Large-scale brain networks and psychopathology: a unifying triple network model. Trends Cognit. Sci. 15 (10), 483–506. https://doi.org/10.1016/j.tics.2011.08.003.

Meyer, S., Mueller, K., Stuke, K., Bisenius, S., Diehl-Schmid, J., Jessen, F., Kassubek, J., Kornhuber, J., Ludolph, A.C., Prudlo, J., Schneider, A., Schuemberg, K., Yakushev, I., Otto, M., Schroeter, M.L., 2017. Predicting behavioral variant frontotemporal

dementia with pattern classification in multi-center structural MRI data. Neuroimage Clin. 14, 656–662. https://doi.org/10.1016/j.nicl.2017.02.001.
Meyers, A., Buqammaz, M., Yang, H., 2020. Cross-recurrence analysis for pattern matching of multidimensional physiological signals. Chaos 30 (12), 123125. https://doi.org/10.1063/5.0030838.
Northoff, G., Bermpohl, F., 2004. Cortical midline structures and the self. Trends Cognit. Sci. 8 (3), 102–107. https://doi.org/10.1016/j.tics.2004.01.004.
Northoff, G., Heinzel, A., De Greck, M., Bermpohl, F., Dobrowolny, H., Panksepp, J., 2006. Self-referential processing in our brain—a meta-analysis of imaging studies on the self. Neuroimage 31 (1), 440–457. https://doi.org/10.1016/j.neuroimage.2005.12.002.
Pedregosa, F., Varoquaux, G., Gramfort, A., Michel, V., Thirion, B., Grisel, O., Blondel, M., Prettenhofer, P., Weiss, R., Dubourg, V., 2011. Scikit-learn: machine learning in python. J. Mach. Learn. Res. 12, 2825–2830.
Pentari, A., Tzagkarakis, G., Tsakalides, P., Simos, P., Bertsias, G., Kavroulakis, E., Marias, K., Simos, N.J., Papadaki, E., 2022. Changes in resting-state functional connectivity in neuropsychiatric lupus: a dynamic approach based on recurrence quantification analysis. Biomed. Signal Process. Control 72, 103285. https://doi.org/10.1016/j.bspc.2021.103285.
Qin, P., Northoff, G., 2011. How is our self related to midline regions and the default-mode network? Neuroimage 57 (3), 1221–1233. https://doi.org/10.1016/j.neuroimage.2011.05.028.
Rachakonda, S., Egolf, E., Correa, N., Calhoun, V., 2007. Group ICA of fMRI toolbox (GIFT) manual. Dostupnez [cit 2011-11-5].“.
Ragland, J.D., Moelter, S.T., Bhati, M.T., Valdez, J.N., Kohler, C.G., Siegel, S.J., Gur, R.C., Gur, R.E., 2008. Effect of retrieval effort and switching demand on fMRI activation during semantic word generation in schizophrenia. Schizophr. Res. 99 (1-3), 312–323. https://doi.org/10.1016/j.schres.2007.11.017.
Raichle, M.E., 2015. The brain's default mode network. Annu. Rev. Neurosci. 38, 433–447. https://doi.org/10.1146/annurev-neuro-071013-014030.
Sambataro, F., Blasi, G., Fazio, L., Caforio, G., Taurisano, P., Romano, R., Di Giorgio, A., Gelao, B., Lo Bianco, L., Papazacharias, A., 2010. Treatment with olanzapine is associated with modulation of the default mode network in patients with Schizophrenia. Neuropsychopharmacology 35 (4), 904–912. https://doi.org/10.1038/npp.2009.192.
Schmitz, T.W., Johnson, S.C., 2007. Relevance to self: a brief review and framework of neural systems underlying appraisal. Neurosci. Biobehav. Rev. 31 (4), 585–596. https://doi.org/10.1016/j.neubiorev.2006.12.003.
Snitz, B.E., Macdonald, A.W., Carter, C.S., 2006. Cognitive deficits in unaffected first-degree relatives of schizophrenia patients: a meta-analytic review of putative endophenotypes. Schizophrenia Bull. 32 (1), 179–194. https://doi.org/10.1093/schbul/sbi048.
Sumiyoshi, C., Ertugrul, A., Anil Yağcıoğlu, A.E., Roy, A., Jayathilake, K., Milby, A., Meltzer, H.Y., Sumiyoshi, T., 2014. Language-dependent performance on the letter fluency task in patients with schizophrenia. Schizophr. Res. 152 (2-3), 421–429. https://doi.org/10.1016/j.schres.2013.12.009.
Sung, K., Gordon, B., Vannorsdall, T.D., Ledoux, K., Schretlen, D.J., 2013. Impaired retrieval of semantic information in bipolar disorder: a clustering analysis of category-fluency productions. J. Abnorm. Psychol. 122 (3), 624–634. https://doi.org/10.1037/a0033068.
Suthaharan, S., 2016. Support vector machine, Machine learning models and algorithms for big data classification. Springer 207–235. https://doi.org/10.1007/978-1-4899-7641-3_9.
Tandon, R., Gaebel, W., Barch, D.M., Bustillo, J., Gur, R.E., Heckers, S., Malaspina, D., Owen, M.J., Schultz, S., Tsuang, M., Van Os, J., Carpenter, W., 2013. Definition and description of schizophrenia in the DSM-5. Schizophr. Res. 150 (1) https://doi.org/10.1016/j.schres.2013.05.028.
Timothy, L.T., Krishna, B.M., Nair, U., 2017. Classification of mild cognitive impairment EEG using combined recurrence and cross recurrence quantification analysis. Int. J. Psychophysiol. 120, 86–95. https://doi.org/10.1016/j.ijpsycho.2017.07.006.
Uddin, L.Q., Clare Kelly, A., Biswal, B.B., Xavier Castellanos, F., Milham, M.P., 2009. Functional connectivity of default mode network components: correlation, anticorrelation, and causality. Hum. Brain Mapp. 30 (2), 625–637. https://doi.org/10.1002/hbm.20531.
Venkataraman, A., Whitford, T.J., Westin, C.-F., Golland, P., Kubicki, M., 2012. Whole brain resting state functional connectivity abnormalities in schizophrenia. Schizophr. Res. 139 (1-3) https://doi.org/10.1016/j.schres.2012.04.021.
Vonk, J.M.J., Rizvi, B., Lao, P.J., Budge, M., Manly, J.J., Mayeux, R., Brickman, A.M., 2019. Letter and category fluency performance correlates with distinct patterns of cortical thickness in older adults. Cereb. Cortex 29 (6), 2694–2700. https://doi.org/10.1093/cercor/bhy138.
Vyas, S., Golub, M.D., Sussillo, D., Shenoy, K.V., 2020. Computation through neural population dynamics. Annu. Rev. Neurosci. 43, 249–275. https://doi.org/10.1146/annurev-neuro-092619-094115.
Wallot, S., 2019. Multidimensional cross-recurrence quantification analysis (MdCRQA) - a method for quantifying correlation between multivariate time-series. Multivariate Behav. Res. 54 (2), 173–191. https://doi.org/10.1080/00273171.2018.1512846.
Wang, H., Zeng, L.-L., Chen, Y., Yin, H., Tan, Q., Hu, D., 2015. Evidence of a dissociation pattern in default mode subnetwork functional connectivity in schizophrenia. Sci. Rep. 5 (1), 1–10. https://doi.org/10.1038/srep14655.
Whitfield-Gabrieli, S., Ford, J.M., 2012. Default mode network activity and connectivity in psychopathology. Annu. Rev. Clin. Psychol. 8, 49–76. https://doi.org/10.1146/annurev-clinpsy-032511-143049.
Woodward, N.D., Cascio, C.J., 2015. Resting-state functional connectivity in psychiatric disorders. JAMA Psychiatry 72 (8), 743–744. https://doi.org/10.1001/jamapsychiatry.2015.0484.
Yan, C.-G., Wang, X.-D., Zuo, X.-N., Zang, Y.-F., 2016. DPABI: data processing & analysis for (resting-state) brain imaging. Neuroinformatics 14 (3), 339–351. https://doi.org/10.1007/s12021-016-9299-4.
Yang, H., 2011. Multiscale recurrence quantification analysis of spatial cardiac vectorcardiogram signals. IEEE Trans. Biomed. Eng. 58 (2), 339–347. https://doi.org/10.1109/TBME.2010.2063704.
Zhang, S., Yang, G., Ou, Y., Guo, W., Peng, Y., Hao, K., Zhao, J., Yang, Y., Li, W., Zhang, Y., Lv, L., 2020. Abnormal default-mode network homogeneity and its correlations with neurocognitive deficits in drug-naive first-episode adolescent-onset schizophrenia. Schizophr. Res. 215, 140–147. https://doi.org/10.1016/j.schres.2019.10.056.
Zhou, L., Pu, W., Wang, J., Liu, H., Wu, G., Liu, C., Mwansisya, T.E., Tao, H., Chen, X., Huang, X., 2016. Inefficient DMN suppression in schizophrenia patients with impaired cognitive function but not patients with preserved cognitive function. Sci. Rep. 6 (1), 1–10. https://doi.org/10.1038/srep21657.